

A peer-reviewed version of this preprint was published in PeerJ on 30 April 2015.

[View the peer-reviewed version](https://doi.org/10.7717/peerj.932) (peerj.com/articles/932), which is the preferred citable publication unless you specifically need to cite this preprint.

Mattei G, Cristiani I, Magliaro C, Ahluwalia A. 2015. Profile analysis of hepatic porcine and murine brain tissue slices obtained with a vibratome. PeerJ 3:e932 <https://doi.org/10.7717/peerj.932>

Profile analysis of hepatic porcine and murine brain tissue slices obtained with a vibratome

This study is aimed at characterizing soft tissue slices using a vibratome. In particular, the effect of two sectioning parameters (i.e. step size and sectioning speed) on resultant slice thickness was investigated for fresh porcine liver as well as for paraformaldehyde-fixed (PFA-fixed) and fresh murine brain. A simple framework for embedding, sectioning and imaging the slices was established to derive their thickness, which was evaluated through a purposely developed graphical user interface. Sectioning speed and step size had little effect on the thickness of fresh liver slices. Conversely, the thickness of PFA-fixed murine brain slices was found to be dependent on the step size, but not on the sectioning speed. In view of these results, fresh brain tissue was sliced varying the step size only, which was found to have a significant effect on resultant slice thickness. Although precision-cut slices (i.e. with regular thickness) were obtained for all the tissues, slice accuracy (defined as the match between the nominal step size chosen and the actual slice thickness obtained) was found to increase with tissue stiffness from fresh liver to PFA-fixed brain. This quantitative investigation can be very helpful for establishing the most suitable slicing setup for a given tissue.

1 **Profile analysis of hepatic porcine and murine brain tissue slices**

2 **obtained with a vibratome**

3 G. Mattei ^a, I. Cristiani ^a, C. Magliaro ^a, and A. Ahluwalia ^{a,b,*}

4 ^aResearch Centre "E. Piaggio", University of Pisa, Largo Lucio Lazzarino 1, 56122 Pisa, Italy

5 ^bInstitute of Clinical Physiology, National Research Council, Via Moruzzi 1, 56124 Pisa, Italy

6 *Corresponding Author

7 Address: Research Centre "E. Piaggio", University of Pisa, Largo Lucio Lazzarino 1, 56122 Pisa,

8 Italy

9 Tel: +39 050 2217050

10 Fax: +39 050 2217051

11 E-mail: arti.ahluwalia@centropiaggio.unipi.it

12 **Keywords:** vibratome, precision-cut slices, liver, brain, graphical user interface

13 1. Introduction

14 Vibrating blade microtomes or vibratomes are commonly used for obtaining precision-cut slices
15 from soft fresh tissues. Unlike classical sectioning procedures based on the use of microtomes,
16 vibratome slicing does not require any tissue fixation, dehydration and embedding thus cell
17 viability and native tissue structure are conserved. Fresh tissue slices are suitable candidates for
18 in-vitro tissue models (Parrish, Gandolfi & Brendel, 1995; Parrish et al., 2002; van de
19 Bovenkamp et al., 2005; Groothuis & de Graaf, 2013) as well as for structural and morphometric
20 analysis (Karim et al., 2013; Eide et al., 2013). For instance, precision-cut liver slices are
21 powerful tools for the in-vitro study of pharmacological metabolism, toxicology and efficacy of
22 novel substances under standardized conditions (van de Bovenkamp et al., 2005, 2006; Van de
23 Bovenkamp et al., 2007; Karim et al., 2013; Eide et al., 2013). They have been used extensively
24 for rank-ordering the toxicity of chemicals and examining the mechanisms of liver injury as well
25 as for investigating the induction of cytochrome P-450 enzymes and the expression of stress
26 proteins or peroxisomal enzymes, thus offering a valuable bridge between in-vivo and cell culture
27 systems (Gandolfi, Wijeweera & Brendel, 1996; Olinga & Schuppan, 2013). Brain tissue slices,
28 on the other hand, are attractive for the evaluation of different morphometric features such as the
29 total extent of dendrites and the number of branching points, as well as for 3D tissue
30 reconstruction and analysis of neurons (Jin et al., 2003; Billeci et al., 2013; Golovyashkina et al.,
31 2014).

32 Despite the widespread use of vibratomes for obtaining live tissue sections, it difficult to find
33 standard preparation protocols or consolidated methods to determine sectioning parameters for
34 generating precision cut slices for a desired application. Thus the purpose of this work was to
35 establish an experimental framework for rapid generation and characterization of precision cut
36 slices without having to resort to lengthy trial and error and tissue wastage. We analyzed tissue

slices from fresh porcine liver and from both PFA-fixed and fresh murine brain. The samples were obtained by varying the two main sectioning parameters, i.e. step size and sectioning speed, to investigate their effect on resultant slice thickness. The other sectioning parameters (i.e. oscillation amplitude and blade angle) were kept constant. To characterize their actual thickness, tissue slices were embedded in agarose gels and sectioned perpendicularly to their surface. The transverse sections were then imaged with an optical microscope and analyzed with a purposely-developed Graphical User Interface (GUI) for semi-automated evaluation of slice thickness.

2. Materials and methods

2.1. Sample preparation and slicing setup

Fresh porcine hepatic tissue was collected from 1 year old healthy pigs and cut into $1.5 \times 0.5 \times 0.5$ cm³ samples, avoiding the Glisson's capsule and macroscopic vasculature. The tissue was obtained from a local abattoir, as a slaughter by-product. Fresh murine brains were collected from n = 2 three month old mice which were deeply anesthetized by intraperitoneal injection of chloral hydrate (400 mg/kg) and then perfused through the left ventricle with 50 mL of 10 mM phosphate buffered saline (PBS 1×, Sigma-Aldrich, Milan, Italy). PFA-fixed brains were obtained from n = 2 three month old mice treated as described for fresh tissue and then perfused with 200 mL of 4 % paraformaldehyde (PFA, pH 7.4) fixative solution prepared in 0.1 M PBS (Sigma-Aldrich, Milan, Italy). Murine brains were cut along to their sagittal plane, obtaining two symmetrical samples. Mouse perfusion was performed at the Department of Translational Research New Technologies in Medicine and Surgery of the University of Pisa. Experiments were conducted in conformity with the European Communities Council Directive of 24 November 1986 (86/609/EEC and 2010/63/UE) and in agreement with the Italian DM26/14. Experiments were approved by the Italian Ministry of Health and Ethic Committee of the University of Pisa.

60 A Leica VT1200 S vibratome (Leica Microsystems, Nussloch, Germany) was used to obtain
61 tissue slices. Each sample was fixed with superglue onto specimen plates and then cut using a
62 stainless steel razor blade (Gillette, Milan, Italy), under buffered conditions with ice-cold PBS
63 1×. The following cutting settings were used: blade angle, 18°; oscillation amplitude, 3 mm for
64 liver, 1.5 mm for brain; sectioning speed, 0.1, 0.2 and 0.4 mm/s for liver, 0.05 and 0.2 mm/s for
65 PFA-fixed brain, step size, 100, 200 and 400 µm. In the case of fresh brain only one sectioning
66 speed (0.2 mm/s) was used on the basis of the results obtained from fixed tissue.

67 2.2. Thickness evaluation

68 The slices obtained were immediately embedded in a 1 % w/v agarose gel (A9539, Sigma-
69 Aldrich, Milan, Italy) prepared in deionized water (Fig. 1). The slice-containing agarose gel,
70 which was formed at room temperature via thermal gelation, allowed an easy and quick
71 embedding of hydrated slices. Notably, this procedure does not require any slice fixation and
72 dehydration unlike classical paraffin embedding. As a consequence there is no tissue collapse or
73 shrinking, hence permitting the evaluation of the actual slice thickness in the hydrated state.

74 To enhance contrast, brain tissue slices were stained with haematoxylin (Sigma-Aldrich, Milan,
75 Italy) prior to embedding (Fig. 1B). Agarose-embedded slices were cut perpendicularly to their
76 surface using a custom slicer and a microtome blade. The cross-sections obtained were placed
77 onto a glass slide and imaged with an Olympus IX81 optical microscope (Olympus, Milan, Italy)
78 at 1.25× magnification. Acquired images were processed with a purposely-developed software
79 implemented in Matlab® (The Mathworks Inc., Natick, MA, USA), named STEGUN (after the
80 mathematician Irene Stegun, the name also stands for “Slice Thickness Evaluation GUI for Non-
81 expert users”, Fig. 2). The software is available for download at

82 <http://www.centropiaggio.unipi.it/software>. STEGUN's simple Graphical User Interface (GUI)

83 allows a semi-automated evaluation of the slice thickness through the following steps:

- 84 1. Set the experimental pixel size ($\mu\text{m}/\text{pixel}$) for image analysis;
- 85 2. Load the image. At this point STEGUN automatically returns the binary image to the user
- 86 who has to select the object representing the slice using the cursor and mouse key;
- 87 3. Rotate the image to vertically align the object, if needed;
- 88 4. Crop three different segments of the object.

89 In particular, the loaded image is binarized through a thresholding algorithm, then the pixel
90 values are inverted to obtain a white object representing the slice (pixel level = 1) in a black
91 background (pixel level = 0). For each of the three crops, the slice thickness is automatically
92 evaluated by summing the pixel values and normalizing the result by the number of pixel rows of
93 the crop. This it is multiplied by the pixel size to obtain the slice thickness in microns. STEGUN
94 stores all the data in a data matrix and displays the result as the mean value \pm standard deviation.
95 In case of highly irregular slices (i.e. when the coefficient of variation, calculated as the ratio of
96 the standard deviation to the mean value, is greater than 0.25) a warning message is returned to
97 the user.

98 **2.3. Data analysis**

99 At least 6 independent tissue slices were analyzed for each step size and sectioning speed
100 investigated. Results are reported as the mean \pm standard deviation, unless otherwise noted. For
101 both porcine liver and PFA-fixed murine brain, the statistical significance between slice
102 thicknesses obtained varying two different sectioning parameters (i.e. step size and sectioning
103 speed) was analyzed using two-way ANOVA. Slice thickness for fresh murine brain was
104 analyzed with one-way ANOVA, since only the slicing step size was varied, keeping the

105 sectioning speed at a constant value. Statistical analysis was implemented in OriginPro 9.0
106 (OriginLab Corporation, Northampton, USA). Differences were considered significant at $p <$
107 0.05.

108 **3. Results and Discussion**

109 **3.1. Fresh porcine liver**

110 We were unable to obtain slices using the 100 μm step size because the blade tended to deform
111 and scrape over the tissue rather than cut it, regardless of the sectioning speed. This is likely due
112 to the very labile and floppy nature of fresh liver (Mattei et al., 2014). Although the two-way
113 ANOVA analysis showed that both the step size and sectioning speed have a significant effect on
114 the resultant thickness of fresh liver slices, 4 of the 6 step size-sectioning speed combinations
115 investigated (specifically 200-0.1, 200-0.4, 400-0.1 and 400-0.2 μm -mm/s) yielded similar slice
116 thicknesses, with an average value of $540 \pm 91 \mu\text{m}$ (Fig. 3A). Moreover, the interaction between
117 the two factors (i.e. step size and sectioning speed) was not found to be significant: lines in Fig.
118 3B exhibit the same trend versus the sectioning speed, regardless of the step size.

119 Overall, although precision-cut liver slices (i.e. with regular and reproducible thickness) were
120 obtained, the slice accuracy (here defined as the match between the nominal step size chosen and
121 the resultant slice thickness obtained) was poor. In particular, the slice thickness was found to be
122 consistently higher than the nominal set step-size selected for slicing the tissue likely because the
123 blade deforms the very floppy and compliant fresh hepatic tissue as it cuts.

124 **3.2. Murine brain**

125 **3.2.1. PFA-fixed brain**

Two-way ANOVA analysis indicates that the thickness of PFA-fixed brain slices depends on the step size only, yielding 3 different groups of slice thicknesses, regardless of the sectioning speed (Fig. 4A). As observed for fresh liver, the interaction between the step size and the sectioning speed was not significant (Fig. 4B).

The thickness of PFA-fixed brain slices matched the nominal step size quite well. This tissue is in fact stiffer than the fresh liver, and hence easier to accurately cut in thin regular slices without significant deformation.

3.2.2. Fresh brain

No slices were obtained using the 100 μm step size, once again because of the floppy and compliant nature of non-fixed soft tissues. One-way ANOVA analysis showed that the resultant thickness of fresh brain slices depends significantly on the step size chosen, with a good match between the two (Fig. 5). These results suggest that, although more compliant than the PFA-fixed tissue, fresh brain is stiff enough to be accurately cut in thin regular slices, unlike the liver.

4. Conclusions

Precision-cut tissue slices from fresh porcine liver as well as from PFA-fixed and fresh murine brain were characterized in their thickness through a semi-automated slice analysis GUI implemented in Matlab[®]. Although precision-cut slices (i.e. with regular and repeatable thickness) were obtained for all the tissues investigated, the results presented in this work suggest that the match between the nominal step size chosen and the actual slice thickness obtained (i.e. slice accuracy) increases with tissue stiffness, from fresh liver to PFA-fixed brain.

146 In conclusion, given the potential benefits and advantages of precision-cut slices in many
147 biological and biomedical engineering applications, the quantitative evaluation of the effects of
148 the vibratome's sectioning parameters on resultant thickness performed in this work can be very
149 helpful for establishing the most suitable slicing setup for a given tissue.

150 **Acknowledgements**

151 The work leading to these results has received funding from the European Union Seventh
152 Framework Programme (FP7/2007-2013) under grant agreement 304961 (ReLiver).

153 **References**

- 154 Billeci L, Magliaro C, Pioggia G, Ahluwalia A. 2013. NEuronMORphological analysis tool: open-
155 source software for quantitative morphometrics. *Frontiers in neuroinformatics* 7:2.
- 156 Van de Bovenkamp M, Groothuis GMM, Draaisma AL, Merema MT, Bezuijen JI, van Gils MJ,
157 Meijer DKF, Friedman SL, Olinga P. 2005. Precision-cut liver slices as a new model to
158 study toxicity-induced hepatic stellate cell activation in a physiologic milieu. *Toxicological*
159 *sciences : an official journal of the Society of Toxicology* 85:632–8.
- 160 Van de Bovenkamp M, Groothuis GMM, Meijer DKF, Olinga P. 2007. Liver fibrosis in vitro: cell
161 culture models and precision-cut liver slices. *Toxicology in vitro : an international journal*
162 *published in association with BIBRA* 21:545–57.
- 163 Van de Bovenkamp M, Groothuis GMM, Meijer DKF, Slooff MJH, Olinga P. 2006. Human liver
164 slices as an in vitro model to study toxicity-induced hepatic stellate cell activation in a
165 multicellular milieu. *Chemico-biological interactions* 162:62–9.
- 166 Eide M, Karlsen OA, Kryvi H, Olsvik PA, Goksøyr A. 2013. Precision-cut liver slices of Atlantic
167 cod (*Gadus morhua*): An in vitro system for studying the effects of environmental
168 contaminants. *Aquatic toxicology (Amsterdam, Netherlands)*.
- 169 Gandolfi AJ, Wijeweera J, Brendel K. 1996. Use of precision-cut liver slices as an in vitro tool
170 for evaluating liver function. *Toxicologic pathology* 24:58–61.
- 171 Golovyashkina N, Sündermann F, Brandt R, Bakota L. 2014. Reconstruction and Morphometric
172 Analysis of Hippocampal Neurons from Mice Expressing Fluorescent Proteins. In: *Laser*

- 173 *Scanning Microscopy and Quantitative Image Analysis of Neuronal Tissue*. Springer, 251–
174 262.
- 175 Groothuis GMM, de Graaf IAM. 2013. Precision-cut intestinal slices as in vitro tool for studies
176 on drug metabolism. *Current drug metabolism* 14:112–9.
- 177 Jin X, Hu H, Mathers PH, Agmon A. 2003. Brain-derived neurotrophic factor mediates activity-
178 dependent dendritic growth in nonpyramidal neocortical interneurons in developing
179 organotypic cultures. *The Journal of neuroscience : the official journal of the Society for*
180 *Neuroscience* 23:5662–73.
- 181 Karim S, Liaskou E, Hadley S, Youster J, Faint J, Adams DH, Lalor PF. 2013. An in vitro model
182 of human acute ethanol exposure that incorporates CXCR3- and CXCR4-dependent
183 recruitment of immune cells. *Toxicological sciences : an official journal of the Society of*
184 *Toxicology* 132:131–41.
- 185 Mattei G, Tirella A, Gallone G, Ahluwalia A. 2014. Viscoelastic characterisation of pig liver in
186 unconfined compression. *Journal of biomechanics* 47:2641–6.
- 187 Olinga P, Schuppan D. 2013. Precision-cut liver slices: a tool to model the liver ex vivo. *Journal*
188 *of hepatology* 58:1252–3.
- 189 Parrish AR, Gandolfi AJ, Brendel K. 1995. Precision-cut tissue slices: applications in
190 pharmacology and toxicology. *Life sciences* 57:1887–901.
- 191 Parrish AR, Sallam K, Nyman DW, Orozco J, Cress AE, Dalkin BL, Nagle RB, Gandolfi AJ.
192 2002. Culturing precision-cut human prostate slices as an in vitro model of prostate
193 pathobiology. *Cell biology and toxicology* 18:205–19.

Figure 1

Agarose-embedded tissue slices.

(A) Fresh porcine liver. (B) PFA-fixed murine brain.

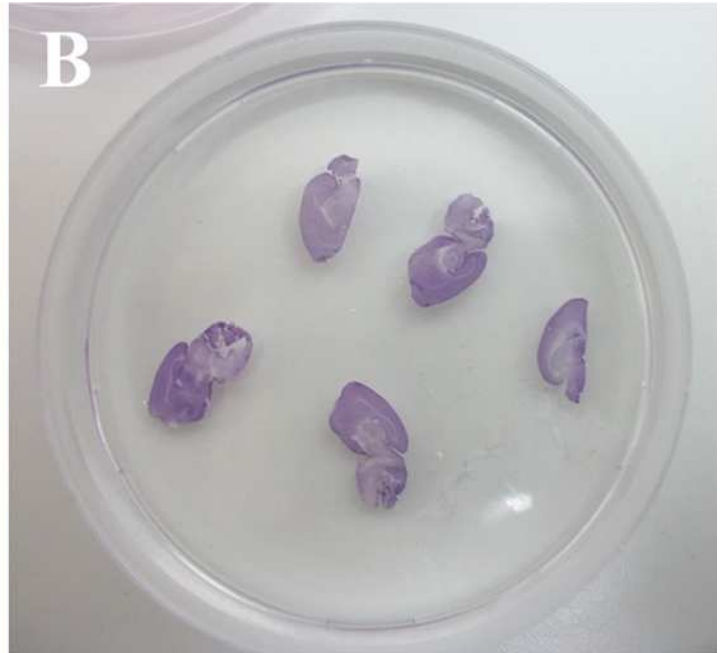
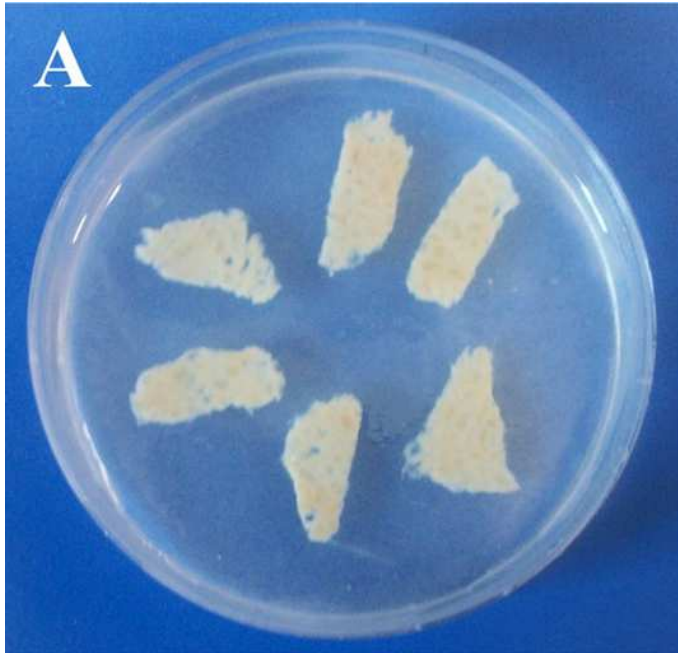


Figure 2

STEGUN: a semi-automated GUI to evaluate slice thickness.

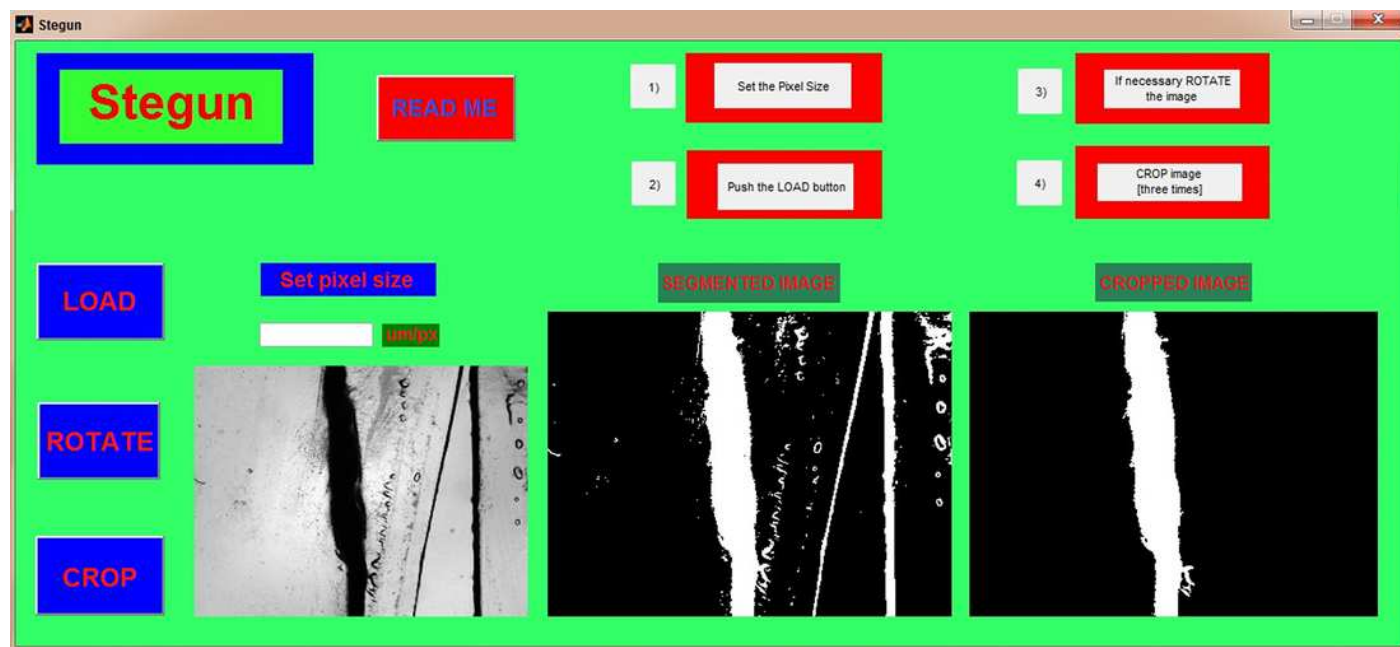


Figure 3

Fresh liver slice thicknesses.

(A) Bar plot: different letters indicate significant differences between samples ($p < 0.05$). Different bar fillings indicate different step sizes. (B) Two-way ANOVA interaction plot: the interaction between the step size and the sectioning speed is not significant.

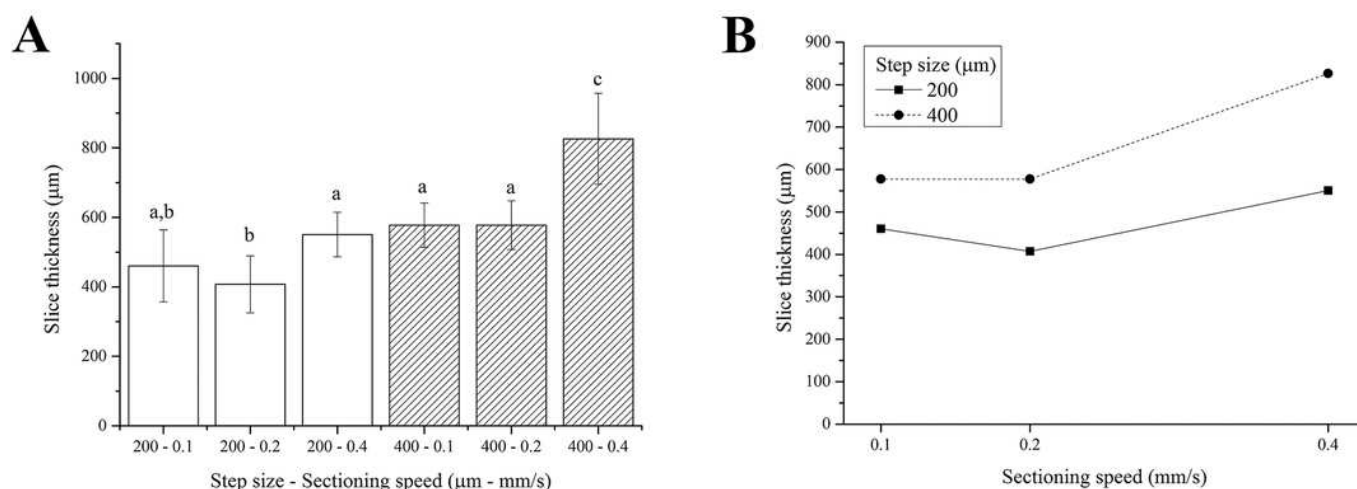


Figure 4

PFA-fixed brain slice thicknesses.

(A) Bar plot: different letters indicate significant differences between samples ($p < 0.05$). Different bar fillings indicate different step sizes. (B) Two-way ANOVA interaction plot: the interaction between the step size and the sectioning speed is not significant.

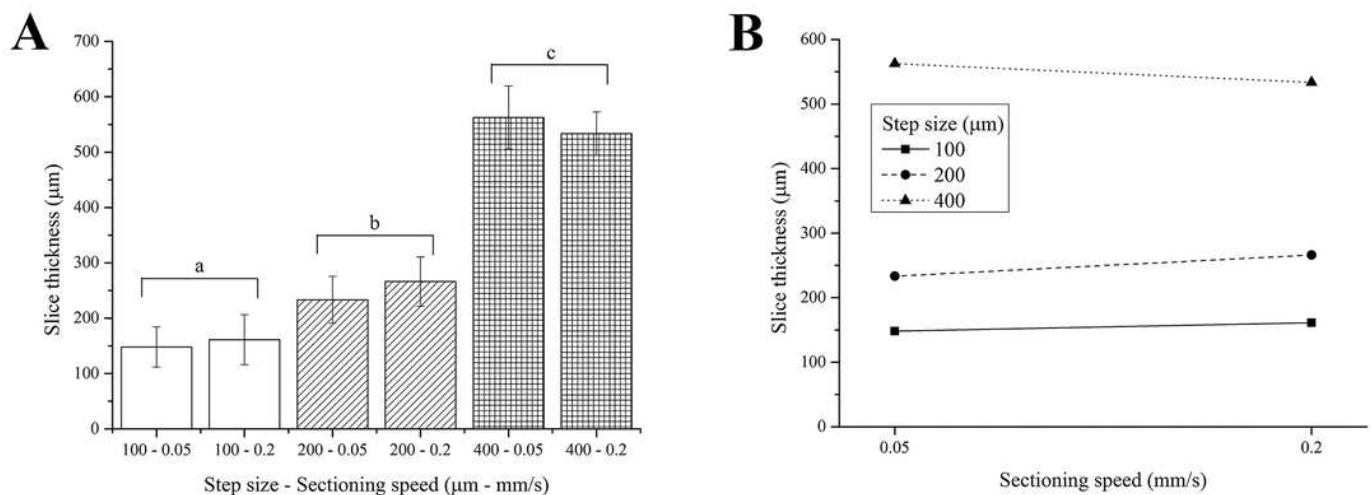


Figure 5

Fresh brain slice thicknesses.

Bar plot: different letters indicate significant differences between samples ($p < 0.05$).

Different bar fillings indicate different step sizes.

